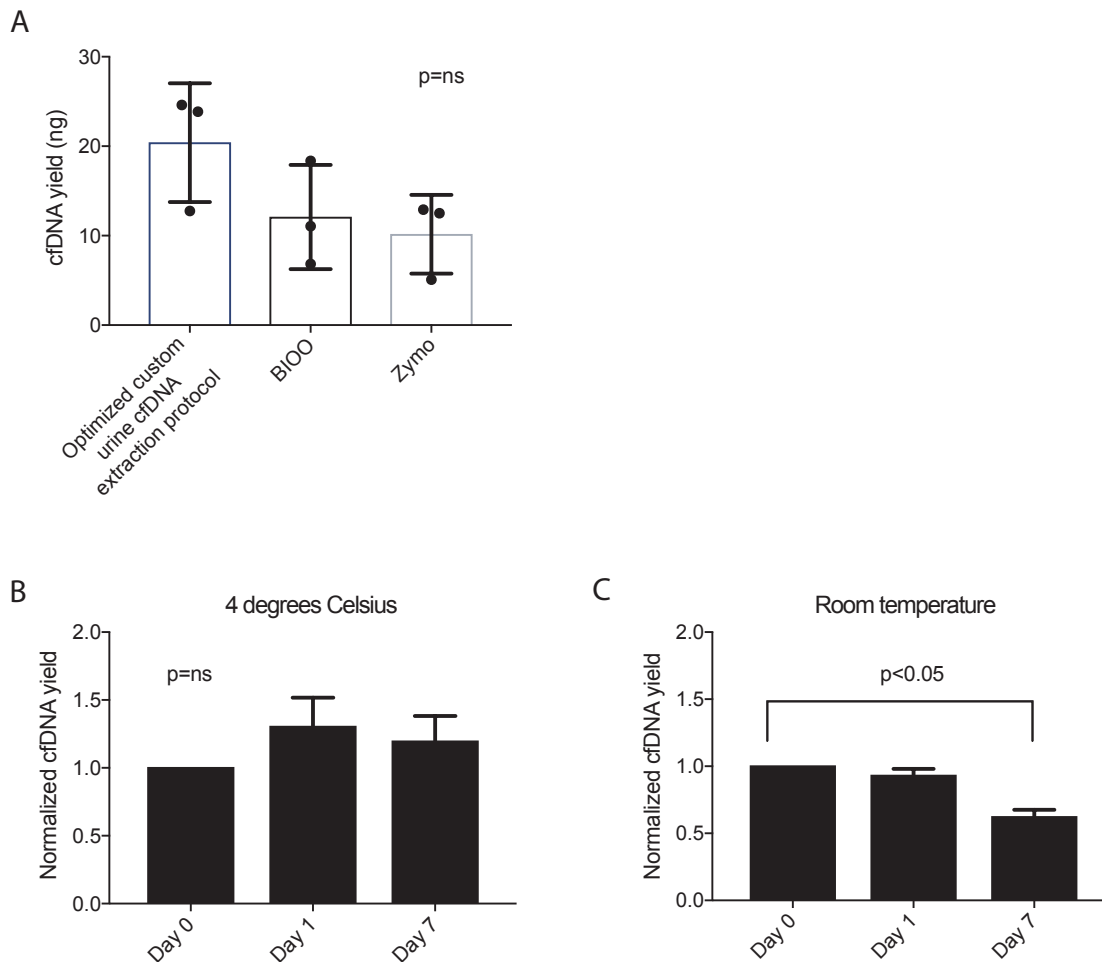
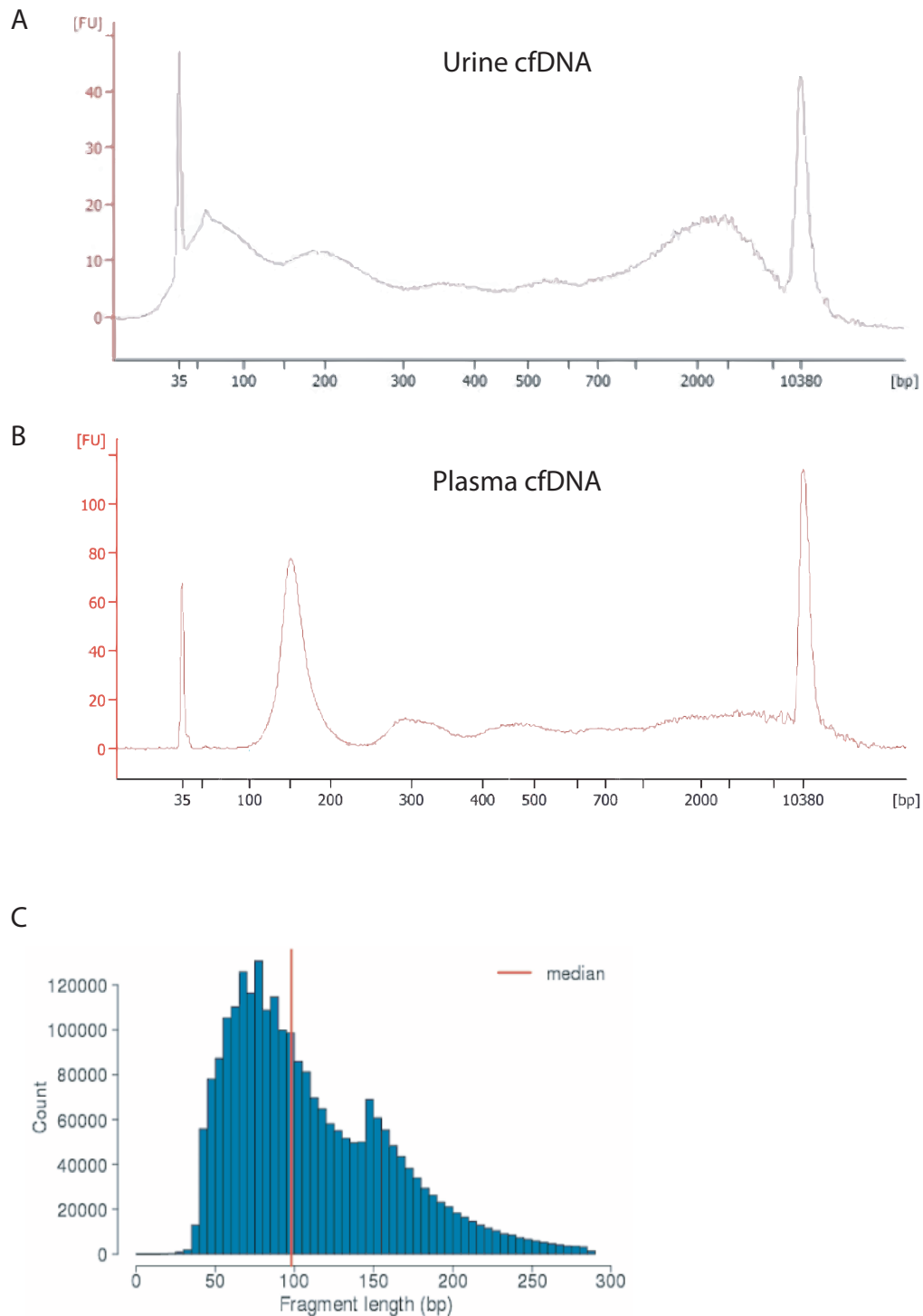


Supplemental Figure S1



Supplemental Figure S1. Optimization of urine cell-free DNA extraction and preservation. (A) Comparison of cfDNA yield by extraction protocol. Three biological replicates were split equally into three aliquots and extracted by our adapted protocol using Q Sepharose (GE Healthcare, Chicago, IL) and by commercially produced kits for urine cfDNA extraction from Bioo (Bioo Scientific, Austin, TX) and Zymo (Zymo Research, Irvine, CA). Urine cfDNA concentrations were analyzed by the double-stranded DNA high sensitivity Qubit kit. Preservation of urine cell-free DNA with 0.5 M EDTA at (B) 4 degrees Celsius for up to seven days and (C) at room temperature. Three biological replicates were processed at each time point. P-values were calculated by one-way repeated-measures ANOVA with the Tukey test to correct for multiple comparisons.

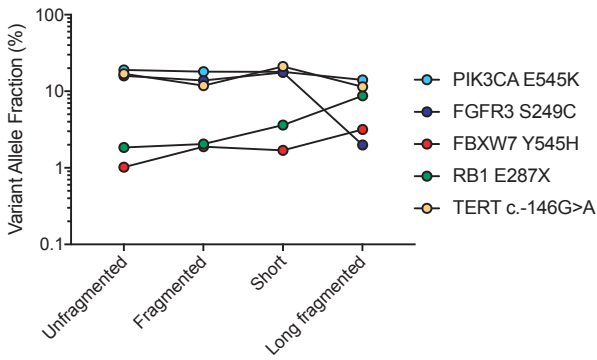
Supplemental Figure S2



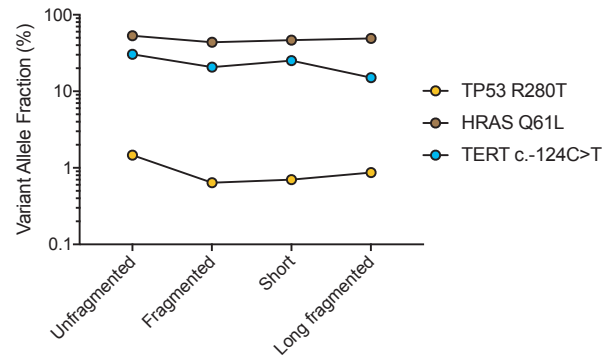
Supplemental Figure S2. Broad distribution of fragment sizes in urine cfDNA versus plasma. Distribution of fragments present by bioanalyzer tracing in (A) a representative urine cfDNA extract from a bladder cancer patient and (B) a representative plasma cfDNA extract from a lung cancer patient. A substantial proportion of fragments urine cfDNA are under 100bp, both in the extract and (C) after enzymatic fragmentation and sequencing.

Supplemental Figure S3

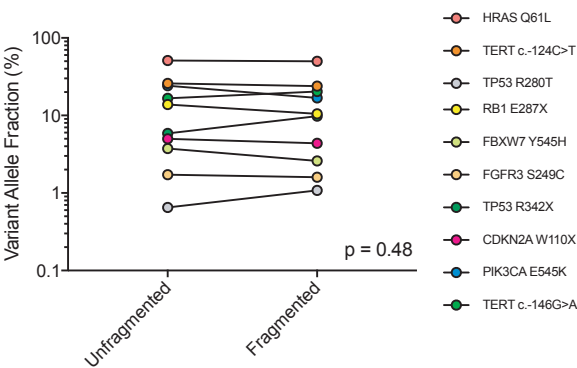
A



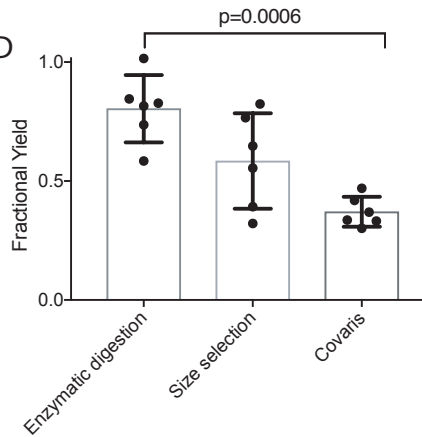
B



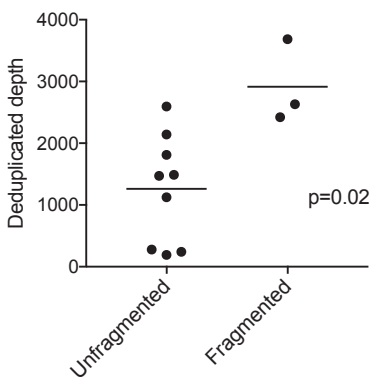
C



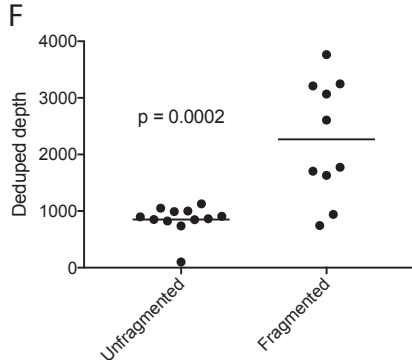
D



E

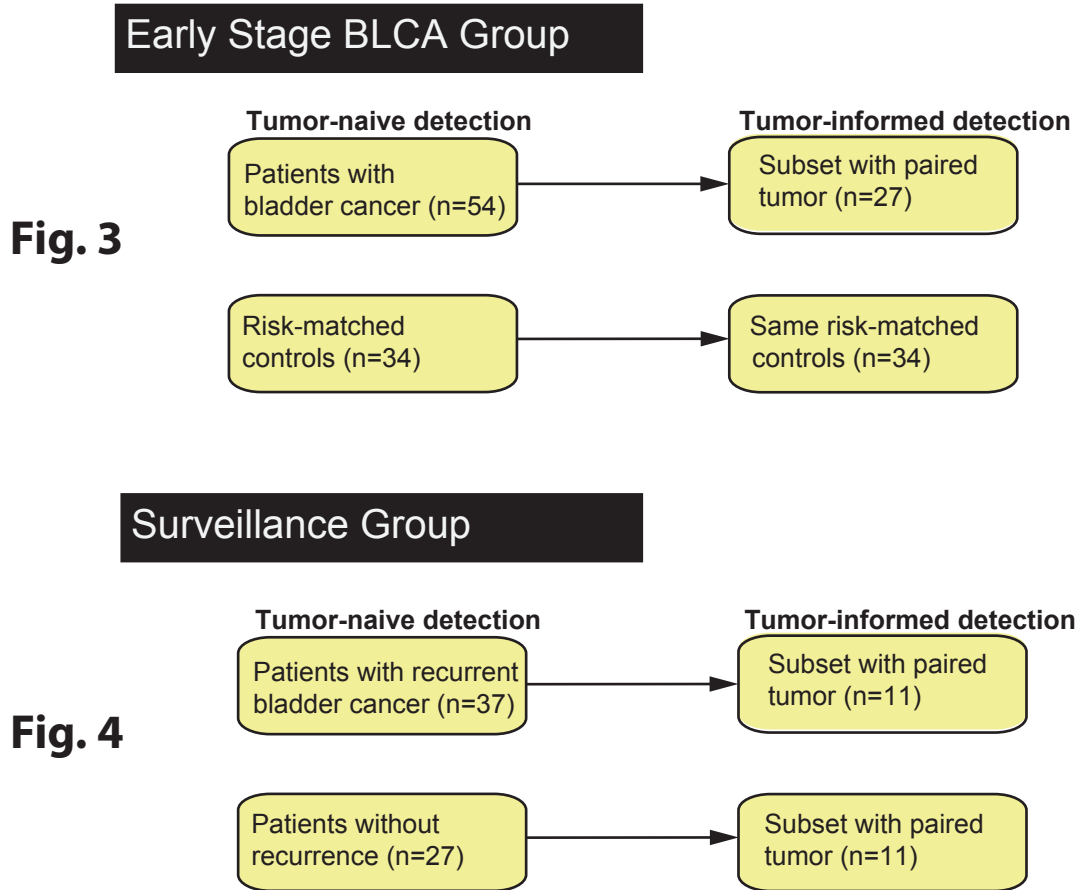


F



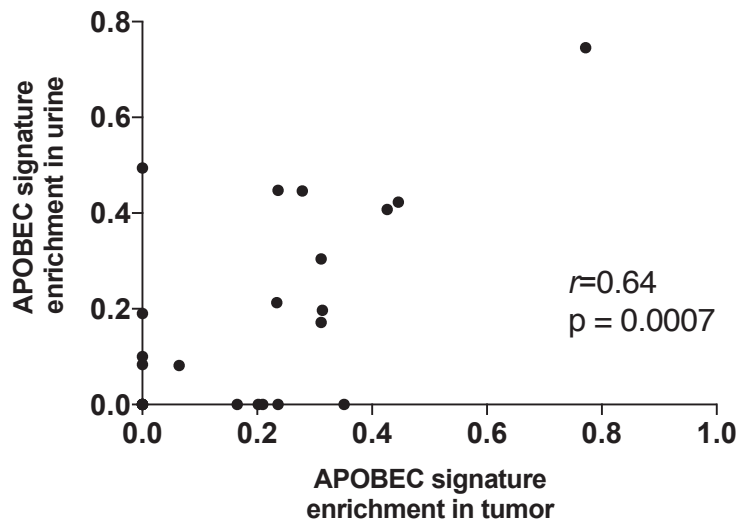
Supplemental Figure S3. Optimization of fragment size selection for urine cell-free DNA profiling. (A-B) Similar variant allele fraction for putative driver mutations in total unfragmented, total enzymatically fragmented, short (<500bp), and long (>500bp) but enzymatically fragmented urine cfDNA from two patients with known bladder cancer. (C) Similar variant allele fractions for putative driver mutations in unfragmented and acoustically fragmented cfDNA from three patients with known bladder cancer. P-value was calculated by paired student's t-test. (D) Comparison of cfDNA yield after enzymatic fragmentation, dual-sided size selection with SPRI select beads (0.6x-2.0x), and acoustic fragmentation. P-value was calculated by one-way repeated measures ANOVA with the Tukey test to correct for multiple comparisons. Superior deduplicated sequencing depth for enzymatically fragmented urine cfDNA sequenced (E) within the same lane as unfragmented cfDNA and (F) in a separate lane. P-values were calculated by the student's unpaired t-test with Welch's correction.

Supplemental Figure S4



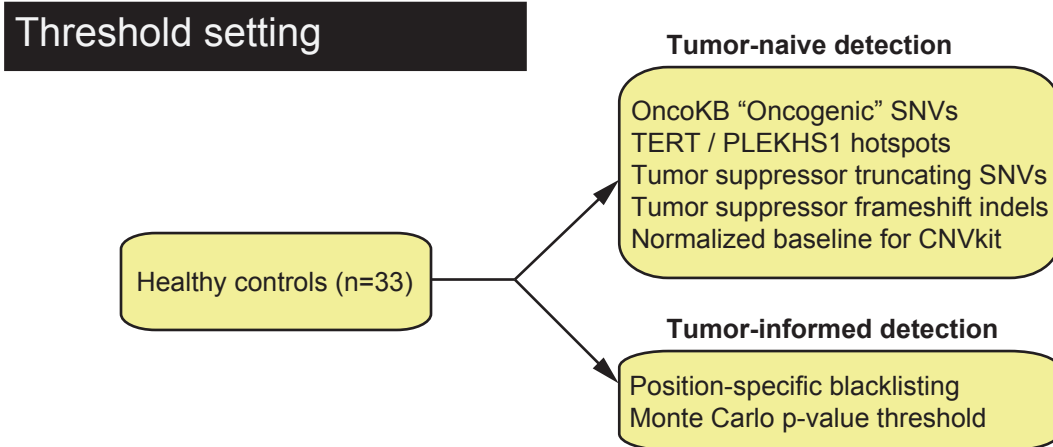
Supplemental Figure S4. Schematic of patient groups and analysis workflow.

Supplemental Figure S5



Supplemental Figure S5. High concordance between urine cfDNA and paired tumor for the APOBEC mutation signature. APOBEC mutational signature enrichment was assessed via the deconstructSigs R package across both synonymous and non-synonymous mutations in cfDNA and concordance was assessed in a subset of patients with active bladder cancer and paired tumor available ($n=24$, Pearson $r = 0.64$, $P = 0.0007$).

Supplemental Figure S6



Supplemental Figure S6. Thresholds for variant calling. Thresholds for variant-calling were set on urine cfDNA from an independent group of 33 young, healthy controls.